

## Thermal equilibrium in proton induced reactions

David H. Boal and James H. Reid

*Theoretical Science Institute, Department of Physics, Simon Fraser University,  
Burnaby, British Columbia, Canada V5A 1S6*

(Received 6 September 1983)

The thermal model, which has been applied successfully to inclusive cross sections in heavy ion reactions, is applied here to the  $(p,p')$  and  $(p,\pi)$  reactions. The thermal source temperatures and velocities determined in proton induced reactions are similar to those found in heavy ion reactions, although the temperatures are cooler in proton induced reactions. Several methods can be used to estimate the number of nucleons in the thermal source, and these are found to give roughly consistent answers. Using a classical dense gas model, an estimate is made of the lifetime of the hot source. As one might expect, the lifetime is calculated to be in the  $10^{-23}$  sec range, indicating that the hot region probably does not cleanly separate from the nucleus before it cools off. A discussion of the limiting temperature behavior observed in this analysis is also given.

### I. INTRODUCTION

The determination of the mechanism for proton induced inclusive reactions resulting in energetic particle emission has proven to be a difficult task. On the one hand, the existence of quasifree peaks in the inclusive cross section of the  $(p,p')$  reaction<sup>1,2</sup> suggests a mechanism<sup>3-5</sup> in which the nonquasifree cross section is attributed to the smearing of the quasifree region by the Fermi motion of the nuclear constituents. On the other hand, the similarity between the measured cross sections of proton induced and heavy ion induced reactions suggests a mechanism like the fireball model<sup>6</sup> of heavy ions, in which there are so many NN scatterings that the inclusive spectra are dominated by phase space effects.

In an effort to sort out the relative contributions of each of these models,  $(p,2p)$  coincidence experiments were performed<sup>7-11</sup> at 198, 300, 640, and 800 MeV incident proton kinetic energy. Typical trigger proton energies were greater than 50 MeV, safely beyond the conventional evaporation regime. The experiments were oriented towards looking for the knockout or direct interaction component of the inclusive reaction mechanism; that is, the experiments included in their kinematic domain, the region in which a fast forward proton is observed with most of the incident proton's kinetic energy save that which is carried off by the trigger and, perhaps, one other accompanying nucleon. Low mass number targets were chosen so as to minimize the effects of multiple scattering not directly associated with the main event which ejected the trigger proton. The experiments confirmed the existence of a knockout contribution to the  $(p,p')$  inclusive reaction for trigger protons with energies beyond the conventional evaporative region, as exemplified in Fig. 1. The magnitude of the contribution appears to be a function of trigger energy and angle.<sup>8</sup> Because of the low event rate, the experiments generally chose trigger angles forward of  $120^\circ$ . It was found that on the order of tens of percent of the inclusive reaction rate could be accounted for in the coincidence experiments. (For details, the interested reader is

referred to the experimental papers themselves.)

However, the experiments also showed that a mechanism in which the residual nucleus recoiled coherently with little excitation energy was not a major contributor. Taking data from the 300 MeV TRIUMF experiment,<sup>8</sup> for example, Fig. 2 shows evidence for both a near coherent peak at combined trigger plus forward proton kinetic energy, not much lower than the incident proton kinetic energy, and a continuum region which looks more like (but is not equal to) what one would expect from the phase space of a residual system which has broken up. The solid curves in Fig. 2 are from a model<sup>12</sup> for the  $(p,p')$  and  $(\gamma,p)$  reactions in which there has been a direct p-N interaction accompanied by breakup of the residual nucleus. While the model's predictions have not been particularly well verified by this experiment, the general two component nature of the model has. A phase space plus direct interaction model has also been used<sup>13</sup> to analyze with success one of the 800 MeV experiments.

The fact that the coincidence experiments do see a phase spacelike component even in the knockout model kinematic regime suggests that statistical or thermal models have a role to play in proton as well as heavy ion induced reactions. The purpose of this paper will be to apply such models to proton induced reactions on both low and high mass targets, in order to determine the model's applicability in these reactions. Sections II and III will deal with some consistency checks which one can use to test the applicability of thermal models. In Sec. IV,

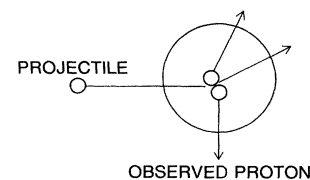


FIG. 1. Model of a knockout component for the  $(p,p')$  reaction.

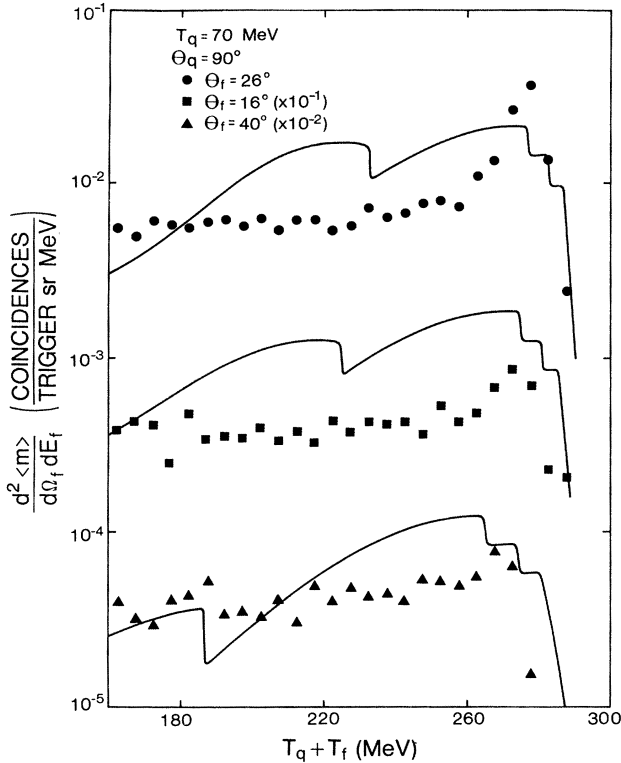


FIG. 2. Comparison of a direct knockout model prediction for the differential multiplicity measured in the TRIUMF experiment. The forward proton's kinetic energy and angle (with respect to the beam direction on the opposite side from the trigger) are defined as  $T_f$  and  $\theta_f$ , while the corresponding quantities for the trigger are  $T_q$  and  $\theta_q$ .

the question of whether the thermal model parameters determined in these tests are meaningful will be addressed. In particular, the implications of a possible limiting temperature will be discussed in Sec. V. The conclusions will be summarized in Sec. VI.

## II. GEOMETRY AND PHASE SPACE

Only a small subset of the target nucleons will initially be involved in a proton induced reaction. This will be true even if the incident proton strikes the target nucleus at zero impact parameter. Of course, this is in strong contrast to reactions involving heavy ions,<sup>14</sup> where the number of NN collisions, and subsequently the number of participating nucleons, is much larger.

To estimate the number of target nucleons participating in the reaction, the following crude calculation, based on geometrical considerations, can be performed. We will assume that an incident proton will interact with all nucleons within a radius  $r_p$  of a straight line trajectory through the nucleus. The nucleus will be imagined to be a sphere of radius  $R = r_0 A^{1/3}$  and uniform density  $\rho$ . Taking the conventional value for  $\rho$  of  $0.17 \text{ fm}^{-3}$  fixes  $r_0$  at 1.12 fm. At a small impact parameter  $b$ , where the surface of the nucleus is roughly normal to the projectile's trajectory, the number of target nucleons in the interaction

region, which we define as  $N_s(b)$ , is

$$N_s(b) = 2\pi(R^2 - b^2)^{1/2} r_p^2 \rho. \quad (1)$$

We will ignore edge effects and assume that this expression is valid for all  $b$ , so that the impact parameter averaged value of  $N_s$  is

$$N_s = \frac{4}{3} \pi r_p^2 R \rho. \quad (2)$$

Lastly, noting that  $r_p$  and  $r_0$  are roughly equal in magnitude, we equate them and substitute for  $\rho$ , obtaining

$$N_s = A^{1/3}. \quad (3)$$

On dimensional grounds alone, one expects to find a proportional sign in Eq. (3), and we see that this simple geometrical model allows the proportional sign to be replaced by an equals sign.

From Eq. (3), one can see that  $N_s$  is small for proton induced reactions. For the targets of interest in the coincidence studies,  $A \simeq 10$ , one finds  $N_s \simeq 2$ , and increases only slowly to about 6 for  $A = 200$ . If  $N_s$  represents the number of nucleons in the initial "hot zone" or thermal source then clearly one must be concerned with the interpretation of thermal model quantities such as temperature. Certainly, for light targets, it is better to deal with phase space explicitly.

In a thermal model for proton induced reactions, one imagines that the projectile gives a certain fraction of its energy and momentum to the  $N_s$  nucleons to form a "hot" source. Depending on the source's velocity and thermal conductivity, questions to which we will return below, the source expands and cools. If the source is moving slowly, most of the energy of the initially hot region may ultimately be dissipated over the entire nucleus, resulting in a nuclear temperature of a few MeV. This latter cool system shows itself in the evaporation of low energy particles (typically less than 10 MeV/nucleon) and its contribution to inclusive spectra is well understood.<sup>15</sup> This paper will concentrate on energetic particle production ( $> 30$  MeV/nucleon) and evidence for a hot zone in these reactions.

As will be shown in the following section on thermal models, the temperatures and velocities of the thermal source estimated from the inclusive spectra indicate that the source size must be small in intermediate energy reactions involving heavy targets. One can use an explicit phase space model to reach the same conclusion.

Our phase space model will assume that the cross section for a given process (here, proton emission in coincidence, inclusive, and integrated measurements) is determined by the phase space available to the  $N$  unobserved recoiling particles.<sup>16</sup> Further, we will work in the intermediate energy regime and assume that  $N$  is sufficiently large that the phase space integral

$$R_N \equiv \int \prod_{i=1}^N \frac{d^3 p_i}{2E_i} \delta^4 \left( K - \sum_i p_i \right) \quad (4)$$

can be approximated by the nonrelativistic expression<sup>17</sup>

$$R_n = \xi_N \left[ \mathcal{M}_k - \sum_{i=1}^N m_i \right]^{(3N-5)/2}, \quad (5)$$

where

$$\xi_N \equiv \frac{(2\pi^3)^{(N-1)/2} \left[ \prod_{i=1}^N m_i \right]^{1/2}}{2\Gamma[3(N-1)/2] \left[ \sum_{i=1}^N m_i \right]^{3/2}}. \quad (6)$$

In these expressions, the  $N$  particle system has overall four-momentum  $K$ , three-momentum  $\vec{k}$ , and invariant mass  $\mathcal{M}_k$ . The masses  $m_i$  of the recoiling particles will all be set equal to the nucleon mass  $m$ , so that

$$R_N = \xi_N (\mathcal{M}_k - Nm)^{(3N-5)/2} \quad (7)$$

and

$$\xi_N = \frac{(2\pi^3)^{(N-1)/2}}{2N^{3/2}\Gamma[3(N-1)/2]} m^{(N-3)/2}. \quad (8)$$

The expression  $R_N$  has an approximate power law behavior for its energy dependence which can be checked experimentally and used to deduce  $N$ . Examining each type of measurement in turn, we have the following:

(i) For the energy and angle integrated cross section, the incident proton is assumed to lose all of its energy and momentum to the  $N_T$  particles which emerge from the target nucleus, as shown in Fig. 3(a). Then, for  $Nm \gg T_p$  ( $T$  will be used for kinetic energy,  $T = E - m$ ),

$$R_{N_T} \approx \xi_{N_T} \left[ \frac{N_T - 1}{N_T} T_p \right]^{(3N_T - 5)/2}. \quad (9)$$

(ii) For the (p,p') inclusive cross section, the incident proton is assumed to lose part of its energy to the observed proton, the remainder being shared by  $N_I$  nucleons recoiling against the observed nuclei [see Fig. 3(b)]. Again, for  $Nm \gg T_p$ :

$$R_{N_I} \approx \xi_{N_I} \left[ \left[ \frac{N_I - 1}{N_I} \right] (T_p - T_q) \right]^{(3N_I - 5)/2}. \quad (10)$$

(iii) Lastly, for the (p,2p) coincidence measurements, the

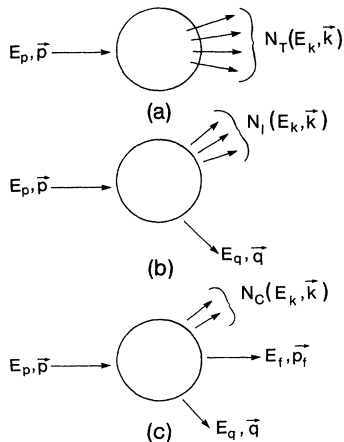


FIG. 3. Kinematic labels for the phase space model of (a) energy and angle integrated cross section, (b) inclusive cross section, and (c) coincidence cross section.

model assumes that  $N_c$  recoiling nucleons carry off that part of the projectile's energy and momentum not taken up by the two observed protons, as shown in Fig. 3(c). Now, we have

$$R_{N_c} \approx \xi_{N_c} \left[ \left[ \frac{N_c - 1}{N_c} \right] (T_p - T_q - T_f) \right]^{(3N_c - 5)/2}. \quad (11)$$

Before we proceed to the determination of these  $N$ 's from data, the use of the projectile energy dependence of the integrated nonevaporative cross section to determine  $N_T$  should be disposed of. Ignoring the energy dependence temporarily, the integrated nonevaporative cross section,  $\sigma(\text{nonevap})$  can itself be used to estimate the source size. For example, we will suppose in Sec. III that the source size is twice the proton multiplicity in the nonevaporative region. One can get this from  $\sigma(\text{nonevap})/\sigma_R$ , the latter being the reaction cross section. However, the reaction cross section is roughly energy independent in the intermediate energy region, so a constant, finite source size would require  $\sigma(\text{nonevap})$  to be constant. This is, in fact, approximately true, as can be seen from Fig. 4. Here,  $\sigma(\text{nonevap})$  per target nucleon for heavy targets has been plotted,  $\sigma(\text{nonevap})$  being determined by numerically integrating the fireball model fits to the nonevaporative inclusive (p,p') spectra, as described in Sec. III. Hence, the integrated cross section has more to do with geometry than phase space, and the cross section's energy dependence is not a useful tool for determining the source size.

The projectile energy dependence of the inclusive spectra is somewhat more promising. Examples of this dependence are shown in Fig. 5, a logarithmic plot of the inclusive (p,p') cross section against  $T_p - T_q$  at fixed observed proton energy and angle. (Detailed phase space model analyses of the ejectile energy dependence at fixed projectile energy were performed some time ago; see Ref. 16.) If all of the increase in the cross section is attributed to the increasing phase space available to the  $N_I$  recoiling particles, then one finds a value for  $N_I$  of 2 to 2.5 for heavy targets. Assuming  $N_T = N_I + 1$ , one sees that the

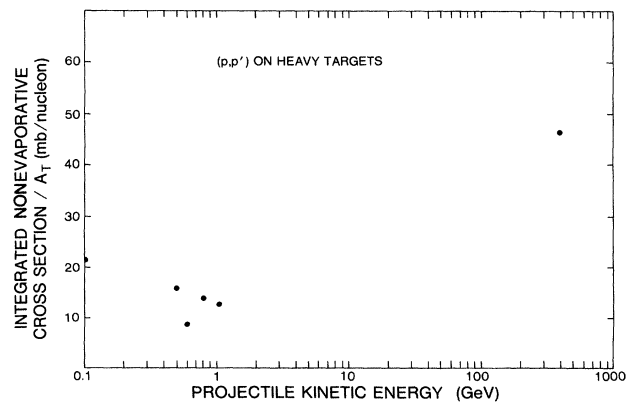


FIG. 4. Integrated nonevaporative cross section per target nucleon for the (p,p') reaction shown as a function of incident proton kinetic energy. The data are for heavy targets.

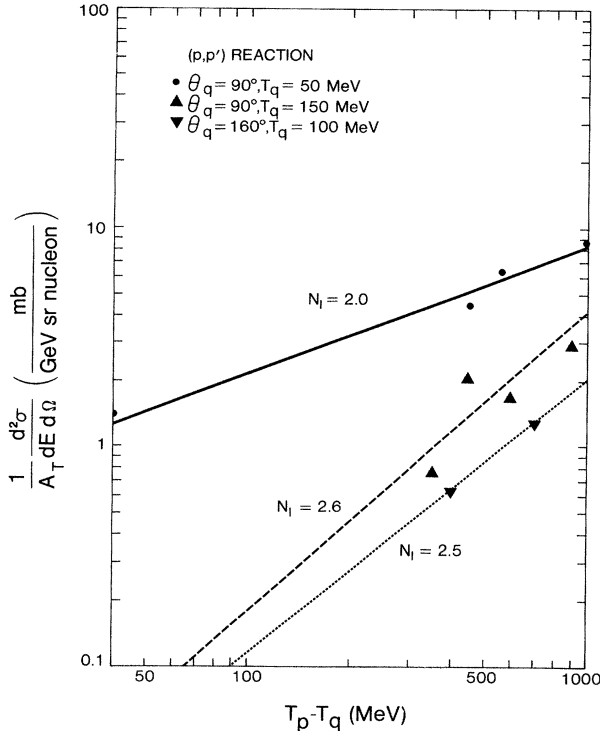


FIG. 5. Inclusive cross section per target nucleon for the  $(p,p')$  reaction at several energies and angles of the observed proton, shown as a function of incident proton energy. The data are from heavy targets.

source is quite small, even smaller than the value of about 6 obtained from geometry. Nevertheless, the interpretation of this approach is clouded by the same problems as were found in  $\sigma(\text{nonevap})$ , namely that the energy dependence of the inclusive cross section is constrained by the condition that its integral should be a constant. Unfortunately there is not enough light target data available to make a good determination as to whether  $N_f$  is smaller for light targets.

The  $T_f$  dependence of the coincidence experiments, at fixed  $T_p$  and  $T_q$ , probably has the fewest interpretational problems. Rather unfortunately, the coincidence measurements are only available for light targets, which are already known<sup>7-11</sup> to show evidence for a knockout component. Because the knockout component shows up as a peak near the kinematic limit at low trigger energies, we will avoid this region in our analysis since phase space obviously will not explain it. Using the  $\text{Be}(p,2p)x$  data, we show in Fig. 6 the dependence of the coincidence rate (here,  $d^2\langle m \rangle / d\Omega_f dE_f$  is the number of coincidences per unit energy and solid angles of the forward proton per trigger) on  $T_f$  at fixed  $T_p$ ,  $T_q$ ,  $\theta_q$ , and  $\theta_f$  [fixed at 300 and 100 MeV,  $90^\circ$  and  $30^\circ$  (on the away side from the trigger), respectively]. The curves are an explicit phase space calculation with two extreme values of  $N_c$  shown, 2 and 8. Clearly, the data favor  $N_c = 2$ .

One can see from the above calculations the values of  $N$  which have been obtained do show evidence for a small source, as expected from geometrical considerations. Of course, one does not expect this model to completely

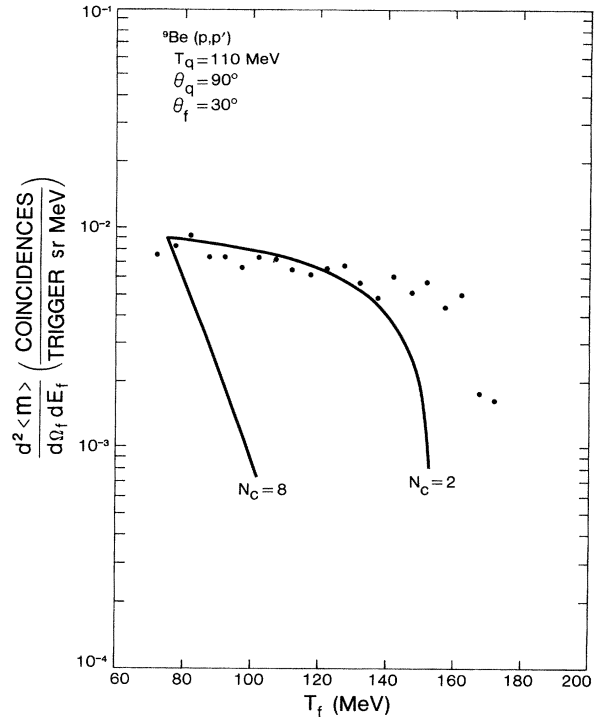


FIG. 6. Differential multiplicity for the  $\text{Be}(p,2p)$  reaction shown as a function of forward proton kinetic energy. The trigger proton energy and angle, as well as the forward proton angle, were held fixed at 110 MeV,  $90^\circ$ , and  $30^\circ$ , respectively. The theoretical curves were normalized to  $9 \times 10^{-3}$  at  $T_f = 75$  MeV.

describe the data, as the coincidence experiments have shown evidence for a knockout component. Nevertheless, the significance of a phase space contribution has been demonstrated. Of course, the small source size is going to add some difficulty to the use of thermodynamic concepts such as temperature. Bearing this caveat in mind, we will now turn to a thermal model analysis of the proton induced reactions involving heavy targets. The results from this analysis will then be contrasted with those obtained in a similar analysis of heavy ion reactions. Thermal models have been applied before to proton induced reactions, particularly by Weiner and co-workers.<sup>18-20</sup> Only a very limited data set was available for analysis in these calculations, and hence, the approach taken was to estimate the model parameters independently and then contrast the model's prediction with data, mainly backwardly produced ejectiles. The approach taken here, in contrast, will be to use a large data set to provide several different determinations of the model parameters, which will then allow for internal consistency checks.

### III. FIREBALL MODEL ANALYSIS

For simplicity, the single fireball model<sup>6</sup> used in heavy ion physics will be used here for a thermal model analysis of proton induced reactions. In this model the non-evaporative part of the inclusive cross section is attributed to emission from a hot source of  $N_s$  nucleons with temperature  $T$  and volume  $V_s$ , which is traveling parallel to the beam with a velocity  $v$ . In the rest frame of the

source, the emission is isotropic and has the form

$$\frac{d^3 n_i}{d^3 q} = g_i \left[ \exp \left[ \frac{E \mp \mu}{T} \right] \pm 1 \right]^{-1}, \quad (12)$$

where  $g_i$  is the number of spin states of the  $i$ th particle species. The  $+1$  ( $-1$ ) on the right-hand side (rhs) refers to fermions (bosons), and in fact will be dropped for the remainder of this paper; i.e., Maxwell-Boltzmann statistics will be used. The chemical potential  $\mu$  will not be used for mesons. A more ambitious calculation would use separate chemical potentials for baryon number, charge, and strangeness, but at these energies only a baryon number chemical potential is required. Here, the  $-$  ( $+$ ) sign of  $\mu$  is associated with baryons (antibaryons) so that  $\mu > 0$  corresponds to a baryon excess. To obtain a cross section from Eq. (12), the number density  $n_i$  will be multiplied by the source volume and the integrated reaction cross section  $\sigma_R$ . This latter step will be used instead of the procedure of integrating  $n$  over impact parameter. In the analysis which is done here, it will be shown that  $T \ll m_p$ , so that nonrelativistic kinematics can be used. Then, defining the total number of particle species  $i$  emitted as  $\mathcal{N}_{i,\text{TOT}}$ , one finds

$$\begin{aligned} \mathcal{N}_{i,\text{TOT}} &= V_s \int \left[ \frac{d^3 n_i}{d^3 q} \right] d^3 q \\ &= g_i V_s e^{(\mu - m_i)/T} \left[ \frac{m_i T}{2\pi} \right]^{3/2}. \end{aligned} \quad (13)$$

This allows us to solve for the chemical potential and remove it from the equations, so that the emission cross section in the source's rest frame can be rewritten as

$$\frac{d^3 \sigma}{d^3 q} = \eta e^{-K_i/T}, \quad (14)$$

where  $K_i$  is the kinetic energy of species  $i$  and

$$\eta = \sigma_R \left[ \frac{1}{2\pi m_i T} \right]^{3/2} \mathcal{N}_{i,\text{TOT}}. \quad (15)$$

One can use two approaches to obtain the parameters in this model from the inclusive data. The first method involves plotting contours of constant Lorentz invariant cross section  $E d^3 \sigma / d^3 q$  as a function of  $q_{\perp}/m$  (where  $q_{\perp}$  is the component of the ejectile's momentum perpendicular to the beam) and rapidity  $y$ , defined by

$$y = \frac{1}{2} \ln \left[ \frac{E + q_{\parallel}}{E - q_{\parallel}} \right], \quad (16)$$

where  $q_{\parallel}$  is the parallel component of the ejectile's momentum.

In the source's rest frame, a contour of constant (Lorentz invariant) cross section at nonrelativistic energies should be semicircular plotted as a function of  $q_{\perp}/m$  and  $y$ , since both of these variables reduce to perpendicular and parallel components of the velocity in the nonrelativistic limit. In transforming to the laboratory frame,  $q_{\perp}/m$  and  $E d^3 \sigma / d^3 q$  are unchanged, of course, and  $y$  is shifted by an amount equal to the rapidity of the source.

Hence, if one makes these plots in the laboratory frame, the source velocity can be determined by finding the centers of the contours. An example of such a plot is shown in Fig. 7. The quasifree contribution in the forward direction has been omitted. One can see that the contours are roughly circular, although relativistic (and other) effects will cause deviations from this shape. Once the source rapidity  $y_s$  is known, then the cross sections can be transformed to the source's frame and both the temperature and  $\mathcal{N}_{i,\text{TOT}}$  determined.

The drawback to this approach is that forward angle data tend to be weighted more heavily than the backward angle data. This is a result of requiring constant cross section as input. The forward angle cross sections tend to be large, so that only a subset of the wide angle data (namely that with large cross sections) can be used to generate a given contour. In a sense, this weighting is reversed to what it should be since the forward angle data include the quasifree region, which is certainly not thermal in origin. Hence, even though we initially used this approach to calculate the model parameters, the results presented here are determined by a different approach which avoids this weighting problem.

This second approach simply fits the laboratory frame data directly with the model, the three parameters being varied in a least squares fit. This is also the approach used in the fits to the heavy ion data which will be presented for comparison. The  $(p,p')$  data are from Refs. 21–27.

In examining the parameters which emerge from the analysis, let us first look at source size. One of the parameters determined by the fitting procedure is  $\eta$ , the  $T_q = 0$  intercept in the source's rest frame. We can use this to invert Eq. (15) to obtain  $\mathcal{N}_{i,\text{TOT}}$ . For simplicity, we will approximate the total reaction cross section<sup>28</sup> by  $\pi R^2$ , since data are not always available for the same energies and targets as are used in the inclusive fits. If, for example,  $\mathcal{N}_{p,\text{TOT}}$  determined in the  $(p,p')$  reaction is equal to the total number of protons in the source, then an estimate of the source size can be obtained. This is shown in Fig. 8(a), where the source size is defined as twice  $\mathcal{N}_{p,\text{TOT}}$ . One finds numbers in the 3 to 4 range, again as is expected

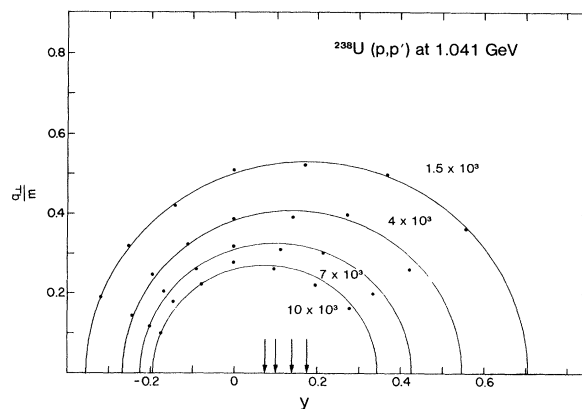


FIG. 7. Circles of constant Lorentz invariant cross section  $E d^3 \sigma / d^3 p$  for the  $U(p,p')$  reaction at  $T_p = 1.041$  GeV. Units are in  $\text{mb/sr GeV}^2$ . Arrows indicate centers of these circles.

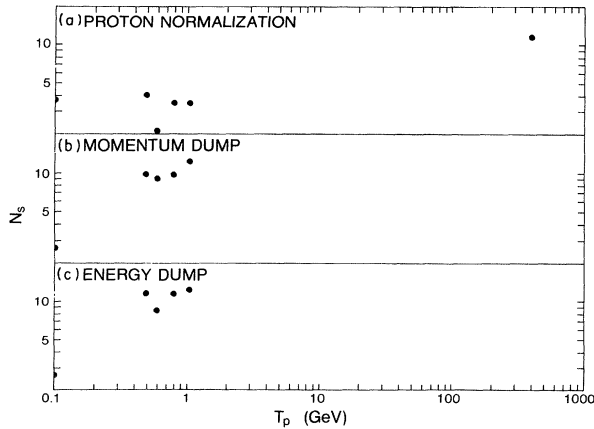


FIG. 8. Estimated number of nucleons in the source (a) from  $(p,p')$  normalization, (b) from momentum dump calculation, and (c) from energy dump calculation. See text for details of the calculations.

from the geometrical calculation.

One can use the source velocities,<sup>29</sup> Fig. 9, to determine how the source was formed. Two calculations will be performed, the first of which we call the momentum dump approach. This calculation assumes that all of the projectile's momentum is lost to the source. One can then take the source rapidity from the fits and, applying conservation of momentum, find the mass of the source. The number of nucleons in the source determined by this approach is shown in Fig. 8(b). One sees that this model for the formation of the source is still in the range expected from geometry, although the source size is as much as double that obtained by the normalization method. We will return to this point below.

An alternative approach, which will be called the energy dump calculation, uses both the source rapidity and temperature<sup>29</sup> (see Fig. 10). Similar to the previous approach, the calculation assumes that all of the incident proton's kinetic energy is converted into translational and

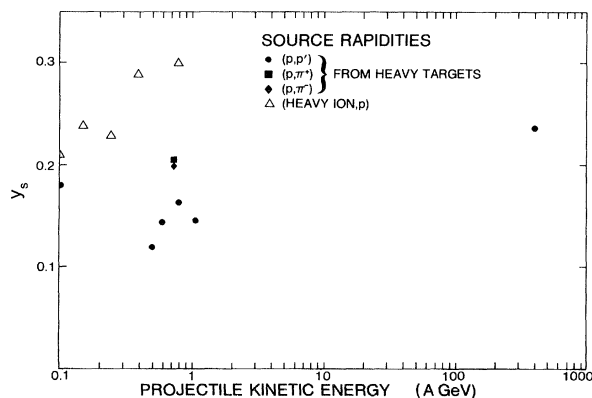


FIG. 9. Source rapidities determined from the  $(p,p')$  and  $(p,\pi)$  reactions. The data are from targets in the mass 200 region, except for the 100 MeV data which was from a nickel target. For comparison, results for proton emission in heavy ion reactions are also shown.

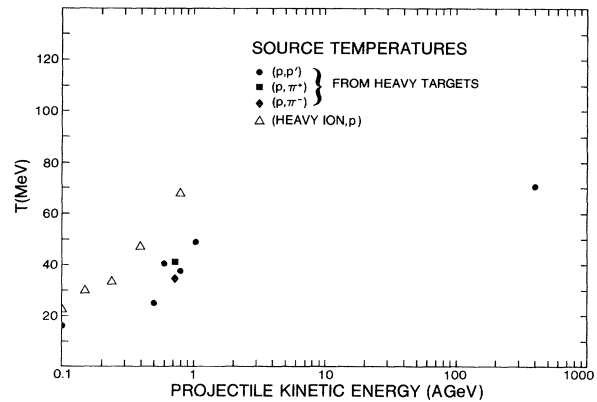


FIG. 10. Source temperatures determined from fits to the  $(p,p')$  and  $(p,\pi)$  data. Data are from heavy targets. For comparison, results for proton emission in heavy ion reactions are also shown.

thermal energy of the source. One sees from Fig. 8(c) that the results from this calculation are consistent with those from the preceding one: the source has about ten nucleons. As with the momentum dump calculation, the calculations agree up to a bombarding energy of a GeV. Beyond this, a comparison is not possible because the projectile's energy and momentum will also be carried by pions, for example. Hence, one would also need normalized pion production data on the same targets, etc., to make a proper comparison.

The fact that the source size, as determined by the  $(p,p')$  normalization technique, is (with the exception of the 100 MeV data) only about half that found by the other techniques may be in part a result of the fact that not all of the nucleons in the source will emerge as free nucleons outside of it: some will emerge as fragments. Similarly, not all of the projectile's energy is necessarily lost to the source. Hence, the energy and momentum dump calculations are in some sense upper bounds, while the normalization calculation is a lower bound. Hence, this factor of 2 disagreement may not necessarily indicate a problem with the thermal model approach.

As an aside, it should be added that the rough consistency which we have obtained with these three calculations on heavy target data is not always found for light target data. One of the worst examples is the  ${}^6\text{Li}$  results<sup>24</sup> at 800 MeV: the three calculations (normalization, momentum, and energy dump) give 1.9, 7.3, and 11.4, respectively, for the number of nucleons in the source. Again, this is what we expect since there is a larger knockout component in the light target data.

To complete this section, an estimate can be made of the volume or density of the hot zone from meson emission. Because the  $(p,\pi)$  reaction is the only one which has been studied with sufficient statistics to perform analysis, it will be the example to be followed through here. For example, the  $\text{Pb}(p,\pi)$  reaction<sup>30</sup> at 730 MeV yields an average ["average" in the sense that the results of the  $(p,\pi^+)$  and  $(p,\pi^-)$  analyses were averaged] temperature and source rapidity of 38 MeV and 0.20, respectively. The

source size, using the energy and momentum dump arguments, is calculated to be 9.6 and 7.3, respectively. These numbers are somewhat smaller than those obtained in the (p,p') reaction. The absolute normalization of the (p, $\pi$ ) reaction can now be used to estimate the source volume. This is because, for mesons, the chemical potential is absent from Eq. (13). The average volume so obtained (that is, with zero chemical potential) is 104 fm<sup>3</sup> for an ideal gas of pions with no decays from higher mass hadrons. Assuming that roughly eight nucleons are contained in this volume, the density at freezeout would be 0.077 fm<sup>-3</sup>. This estimate is similar to that found in heavy ion reactions for a simultaneous fitting of the proton and pion emission data.<sup>31</sup> Before leaving this section, it is worthwhile pointing out that we have ignored that contribution to pion production coming from decay of higher mass baryons such as the  $\Lambda(1232)$ . Inclusion of these species would lower the estimated source volume. We will return to a discussion of the inferred pion temperature in the next section.

#### IV. TIME EVOLUTION OF THE HOT ZONE

It has been demonstrated in the preceding section that several different methods of calculating the source size indicate that the hot region formed in proton induced reactions is fairly small, containing fewer than ten nucleons. Leaving aside the self-consistency problems in these calculations for the moment, another pressing question is: Does the hot zone remain hot long enough for there to be particle emission?

A first attempt at answering this question was made by Weiner and Weström,<sup>18</sup> who made use of calculations of the thermal conductivity of nuclear matter performed decades ago by Tomonaga.<sup>32</sup> The classical diffusion equation for temperature,  $T$ , as a function of time,  $t$ , reads

$$C_p \frac{\partial T}{\partial t} = \text{div} \left[ \frac{\kappa}{\rho} \text{grad} T \right], \quad (17)$$

where  $C_p$  is the specific heat at constant pressure,  $\rho$  is the density, and  $\kappa$  is the thermal conductivity. Since all of these quantities are functions of  $T$  at low temperature, the solution of the diffusion equation is rather complicated. However, Weiner and Weström made the following point: At low temperatures ( $T \ll \epsilon_F$ , the Fermi energy),  $\kappa \propto T^{-1}$ , and  $C_p \propto T$ , so that

$$\frac{\kappa}{\rho C_p} \propto T^{-2}. \quad (18)$$

Thus, one would expect  $\partial T / \partial t$  to decrease as  $T$  increases. While this may be true at low temperatures, it is not relevant at the temperatures considered here, where  $T$  is on the order of  $\epsilon_F$ . In this regime, the thermal conductivity and heat capacity have very different temperature dependence than what is observed at  $T \ll \epsilon_F$ .

In order to estimate the lifetime of the hot zone, we will perform our calculations at  $T = 60$  MeV. This temperature is roughly double  $\epsilon_F$ , and allows us to describe the nucleus with Maxwell-Boltzmann statistics, rather than the Fermi-Dirac statistics needed by Tomonaga at  $T < 10$  MeV. We will assume that the nucleons are rigid spheres

of diameter  $d = 1$  fm and form a nearly ideal gas ( $C_p = \frac{5}{2} k_B$ ,  $C_v = \frac{3}{2} k_B$ , where  $k_B$  is Boltzmann's constant). In the zero-pressure limit, this gas of hard spheres has a thermal conductivity  $\kappa_0$  given by (see, for example, Refs. 33 and 34)

$$\kappa_0 = \frac{25}{32} \left[ \frac{k_B T}{\pi m} \right]^{1/2} \frac{C_v}{d^2}. \quad (19)$$

In Enskog's theory<sup>35</sup> of transport phenomena in dense gases,

$$\kappa / \kappa_0 = (b_0 / \tilde{V}) \left[ \frac{1}{y} + 1.2 + 0.755y \right], \quad (20)$$

where  $\tilde{V}$  is the molar volume,

$$y = \left[ \frac{P \tilde{V}}{RT} - 1 \right], \quad (21)$$

and  $b_0$  is the second virial coefficient. At moderate densities,<sup>23</sup>

$$y = \left[ \frac{b_0}{\tilde{V}} \right] + 0.625 \left[ \frac{b_0}{\tilde{V}} \right]^2 + 0.287 \left[ \frac{b_0}{\tilde{V}} \right]^3 + 0.115 \left[ \frac{b_0}{\tilde{V}} \right]^4. \quad (22)$$

For a hard sphere gas,

$$b_0 / \tilde{V} = \frac{2}{3} \pi \rho d^3. \quad (23)$$

This gives  $\kappa / \kappa_0 = 1.13$  at a density of  $\rho_0 / 2$ . For calculational purposes, we will assume that the temperature profile of the hot source has a Gaussian shape as a function of radius  $r$ :

$$T(r) = T_0 \exp[-(r/r_0)^2]. \quad (24)$$

Of course, the central temperature  $T_0$  will be time dependent. We can estimate how rapidly it changes by assuming that  $C_p$ ,  $\rho$ , and  $\kappa$  are sufficiently slowly varying (as a function of  $r$ ) that Eq. (17) can be rewritten as

$$\frac{\partial T}{\partial t} = \frac{\kappa}{\rho C_p} \nabla^2 T. \quad (25)$$

At  $r = 0$ , this is simply

$$\frac{\partial T}{\partial t} = - \frac{\kappa}{\rho C_p} \frac{6}{r_0^2} T_0. \quad (26)$$

Choosing  $r_0 = 3$  fm, to correspond to a volume of about 100 fm<sup>3</sup> for the hot zone, and  $\rho = \frac{1}{2} \rho_0$  (as estimated from the pion data) we find

$$\partial T_0 / \partial t = -107 \text{ MeV} / (10^{-23} \text{ sec}). \quad (27)$$

This is a very rapid cooling, not at all what one would have found had one assumed that Tomonaga's results applied in this temperature range. For comparison, one can estimate the transit time of the hot sources to emerge from the nucleus. Assuming that the source has to travel a distance of, say, 5 fm at a speed of 0.25c, then the transit time would be  $6.7 \times 10^{-23}$  sec. Clearly, the source

loses its thermal energy, presumably through particle emission, before it leaves the nucleus.

As the temperature drops, so will the rate of cooling. The classical equations which we have used here will no longer be valid. A numerical approach to this temperature regime ( $T \leq 25$  MeV) has been performed by Kohler<sup>36</sup> and much lower cooling rates are observed for the central region. The calculations are not completely comparable with what we have done here because the density chosen was larger and only the one dimensional problem was considered. However, his calculations indicate that the rate of cooling may drop by on the order of a factor of 5 for  $T < 25$  MeV.

For very low temperatures, Tomonaga's result<sup>32</sup> for  $\kappa$  can be used:

$$\kappa = (7/48\pi\sqrt{2})(E_F)^{3/2}/\sqrt{m} TQ, \quad (28)$$

where  $Q$  will be set<sup>36</sup> equal to 13.5 mb. For  $T=5$  MeV and  $r_0=7$  fm, this gives  $\partial T/\partial t=0.6$  MeV/( $10^{-23}$  sec) at  $\rho=\rho_0$ . In summary, we see that the cooling is very rapid at first, but slows down dramatically as one approaches equilibrium of the whole nucleus.

It may be possible to learn about the time evolution of the hot zone by studying the temperature and volume of the source as a function of the mean free path of the ejectile. For example, it has been proposed<sup>14,37</sup> that the ordering of the apparent temperatures observed in heavy ion reactions<sup>38</sup>

$$T^K > T^p > T^\pi, \quad (29)$$

(where the superscript refers to the ejectile which measures the temperature) is related to the mean free path of the ejectile. Long mean free path particles such as the kaon presumably measure the hot interior of the thermal source, while short mean free path particles such as the pion would measure the cooler surface region of the source or the freeze out temperature. A test of this interpretation proposed by Nagamiya<sup>39</sup> would be to use the absolutely normalized cross sections to determine the source volume, as was done here in the (p, $\pi$ ) analysis.

In proton induced reactions, one would expect to see the same trend of temperatures as suggested in Eq. (29), but with much smaller differences. Since the source in proton induced reactions has less than ten nucleons, it probably has no distinct "interior" and hence the pion and proton temperatures should be very similar. Similarly, the initial hot zone probably has a density not much above normal

nuclear matter, so the temperature decrease from expansion of the source from its initial phase (proton thermometer) to the freeze out point (pion thermometer) will also be less than what is expected in heavy ion reactions.

Indeed, this is what one finds experimentally. In heavy ion reactions,  $T^p/T^\pi$  is about<sup>38</sup> 1.2, whereas in proton induced reactions it drops to about unity.

Of course, all of these temperature estimates carry a considerable error. The main source of error probably lies with the inclusion of the forward angle data in the analysis. On the one hand, these data in principle allow one to determine  $T$  and  $y_s$  with more accuracy. On the other hand, they contain the quasifree contribution, which is difficult to extricate from the thermal component. This leads to higher temperatures and source velocities than what one would obtain in the absence of a quasifree contribution.

It is not clear whether temperatures determined from emission of composite particles, d and t, fit into this scheme. Since the deuteron and triton have shorter mean free paths than the proton, one might expect their temperatures to be lower, if they are thermal in origin. This is not observed experimentally: their temperatures are very similar to those found in the (p,p') analysis. Perhaps this is again a reflection of the small source, just as  $T^\pi \simeq T^p$  may be. However, the similarity between  $T^t$ ,  $T^d$ , and  $T^p$  is also what one would expect for fragment production in either the traditional coalescence model<sup>40,41</sup> or the snowball model.<sup>42</sup>

## V. LIMITING TEMPERATURES

The last topic which we wish to examine in this survey of thermal models is the limiting temperature behavior shown in Fig. 10. Here, one sees that the temperature appears to asymptotically approach a limiting value as the bombarding energy is increased. This behavior is also observed in thermal model analyses of both p + p and  $\alpha + \alpha$  collisions,<sup>43</sup> although the limiting temperature is substantially higher than what is observed here. There are many interpretations of such a temperature in terms of statistical phenomena: phase transitions and the density of hadronic states. However, before we address whether this limiting temperature has anything to say about these effects, we wish to show how even a direct knockout model can produce the same behavior.

In the knockout model for the (p,p') reaction, the differential cross section is expressible as<sup>12</sup>

$$\frac{d^3\sigma}{d^3q} = \frac{1}{2^4(2\pi)^5 p E_q} \sum_{i=1}^{A_T-1} \frac{a_i(i+1)}{M_{T_i}} \int \frac{d^3p_f}{E_f} d^4K D_i(k)n(k)(Z_T |t_{pp}|^2 + N_T |t_{pn}|^2) \delta^4(\text{energy momentum}), \quad (30)$$

where  $K$  is the total four-momentum of the recoiling  $i$ -nucleon jet ( $k$  is the three momentum) and the  $D_i$ 's are the recoiling jet invariant mass distributions. The number of protons and neutrons in the target is  $Z_T$  and  $N_T$ , respectively. The quantity  $t_{NN}$  is the elementary nucleon-nucleon transition matrix element. All mass numbers of the recoiling jet are summed over (the kinematic labels are shown in Fig. 11), each being weighted by a coefficient  $a_i$ .

In the plane wave impulse approximation (PWIA) picture,  $n(k)$  is the single nucleon inclusive momentum distribution, and is a function of  $k$ . At large  $k$ , many body calculations,<sup>44,45</sup> and (p,p') phenomenology, show that  $n(k)$  has the form

$$n(k) \propto e^{-k/k_0}, \quad (31)$$

where  $k_0$  is a parameter, generally having a value around



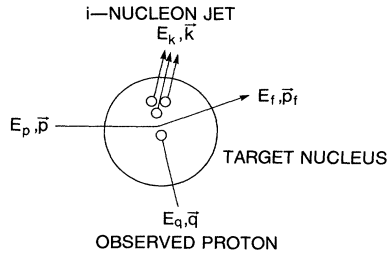


FIG. 11. Kinematical labels used for the direct knockout model of Eq. (30).

100 MeV. One does not need to pursue a full direct knockout model calculation to obtain its dependence on projectile energy. Rather, one can follow Frankel<sup>4,5</sup> and replace the  $D_i$ 's with delta functions, truncate the sum to include only coherent recoil, and assume that the most rapidly varying part of the integral in Eq. (30) is  $n(k)$  because of its exponential nature. Then

$$\frac{d^3\sigma}{d^3q} \propto \exp(-k_{\min}/k_0). \quad (32)$$

In other words, the cross section is dominated by the kinematical situation in which the observed nucleon is required to have the least momentum,  $k_{\min}$ , inside the target nucleus before it is struck. A phase space model will also have a dependence on  $k_{\min}$ , although it will be different.

At fixed ejectile energy and angle,  $k_{\min}$  will decrease to constant value as the incident energy increases. Hence, the cross section will increase to a constant value as the incident energy increases; this is shown in Fig. 12. This simplified knockout model would predict that the differential cross section should become roughly constant as a function of bombarding energy in the few GeV region. Hence, a thermal model analysis of a reaction which is actually knockout in origin will yield a constant temperature

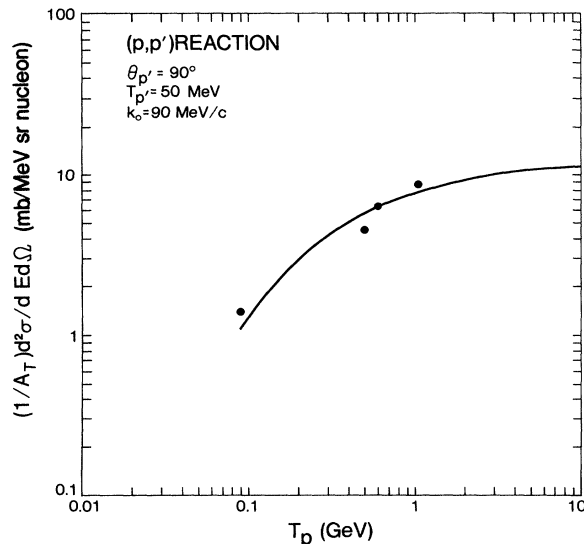


FIG. 12. Behavior of  $\exp(-k_{\min}/k_0)$  for  $T_q$  and  $\theta_q$  fixed at 50 MeV and  $90^\circ$ , respectively. The parameter  $k_0$  has been assigned a value of 90 MeV/c.

in the same kinematical region.

Now that it has been established that the knockout component of the inclusive reaction mechanism will approach a limiting value in the few GeV region, let us examine what aspects of a thermal model will do the same. There are several possibilities, among them the following: (i) nuclear matter is undergoing a phase transition; (ii) production of higher mass hadrons is consuming energy without increasing the temperature, and (iii) elementary nucleon-nucleon kinematics is preventing the further deposition of energy beyond the few GeV range. Each of these possibilities will be examined in turn.

The most likely phase transition in the few GeV region would be that from hadronic to quark matter. A simple estimate of the latent heat of the transition which uses some aspects of the bag model yields<sup>46</sup>

$$L = 4B, \quad (33)$$

where the bag constant  $B$  has a value of about  $(160 \text{ MeV})^4$ . This gives a latent heat of about  $340 \text{ MeV}/\text{fm}^3$ , meaning that at least 12 GeV would have to be put into the initial hot zone ( $\sim 35 \text{ fm}^3$ ) before the temperature could rise further. This by itself would not account for the flattening of the temperature over the few hundreds of GeV of bombarding energy indicated by Fig. 10, unless mechanisms (ii) or (iii) were operating as well.

The ordering of the temperatures in proton versus heavy ion reactions is also opposite to what one would expect for the quark-hadron transition. Calculations consistently show<sup>47</sup> that the transition temperature decreases with increasing baryon number density. Since one would expect a heavy ion collision to achieve a higher baryon number density than a proton induced reaction,<sup>48</sup> the heavy ion transition temperature should be lower than the proton one. This is opposite to what is observed for the asymptotic region of Fig. 10.

The second mechanism relies on the roughly increasing density of states of the hadronic mass spectrum to allow the hot zone to absorb more of the projectile's energy and momentum without increasing the temperature. An early model<sup>49</sup> of the hadronic mass spectrum which had an exponentially increasing density of states gave a limiting temperature of about  $m_\pi$ , substantially higher than that which is observed here. Further, one would expect to find the same limiting temperature in both proton and heavy ion reactions. Thus, the role of mechanism (ii) is probably simply to slow down the increase in temperature as more energy is added to the system.

Mechanism (iii), we suspect, is the main reason for the limiting behavior of the cross sections. In mechanism (iii) the energy dependence of elementary nucleon-nucleon scattering limits the amount of energy lost per NN collision, and hence the temperature which can be obtained. The intranuclear cascade calculation which would be required to support this hypothesis is beyond the scope of this paper, but one can perform a fairly simple calculation to show the effect. Using elastic scattering cross sections only, Fig. 13 shows the result of an estimate of the mean energy loss per NN collision. That is, the elastic cross section was taken to have the usual parametric form<sup>50</sup>

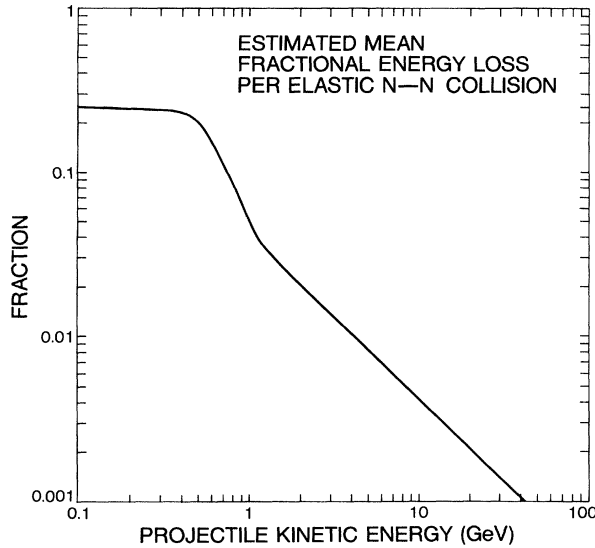


FIG. 13. Estimated mean fraction of energy lost per NN collision for elastic scattering.

$$\frac{d\sigma}{dt} = Ae^{bt}, \quad (34)$$

where  $A$  and  $b$  are parameters and  $t$  is the four-momentum transfer. Then,  $\bar{t}$  was found such that half of the integrated cross section lay between  $0 \geq t \geq \bar{t}$  and half between  $\bar{t} \geq t \geq 4m_N^2 - s$ , where  $s$  is the center of mass energy squared. The energy lost in the laboratory frame corresponding to this  $\bar{t}$  is plotted in Fig. 13. One can see that, for incident energies less than 500 MeV or so, about three collisions of the incident nucleon would be required for it to lose most of its energy. Using  $(\rho\sigma)^{-1}$  for the mean free path, an average over impact parameter yields about three for the average number of interactions of the projectile. Hence, in this energy range one expects the projectile, on average, to lose a substantial fraction of its energy and momentum to the hot zone. As the incident energy increases past 1 GeV, the average energy loss, like the total cross section, tends to a constant. Hence, in the high energy region, the projectile loses a constant amount of energy to the source, almost independent of projectile energy. This calculation has omitted inelastic effects which will increase the energy loss at high pion multiplicities, but the general effect should remain the same.

To summarize, the limiting temperature effect seen in proton induced reactions probably lies less with phase transitions than simple NN dynamics which curtail the energy loss per NN collision at high bombarding energies.

## VI. SUMMARY

The role of statistical mechanisms for proton induced reactions resulting in the production of protons and pions has been investigated. Geometrical arguments lead one to

believe that the number of participants in the reaction is small, perhaps only six nucleons even in mass 200 targets. This conclusion is borne out in a phase space model analysis of the energy dependence of the inclusive and coincidence cross sections. In this model, the cross section has a power law dependence on energy, the exponent of the power law allowing a determination of the number of participating particles. Less than five participating nucleons are indicated in this model analysis.

Notwithstanding the difficulties of dealing with the interpretation of a statistical ensemble of fewer than ten particles, a thermal model analysis of heavy target  $(p,p')$  and  $(p,\pi)$  reactions was undertaken. The results showed a consistent picture for bombarding energies of less than a GeV in which the projectile loses most of its kinetic energy and momentum to a small number (4–12) of nucleons which form an equilibrated source, although the model is only roughly self-consistent. The  $(p,\pi)$  reaction allows one to determine the source volume, which, when combined with the source mass estimates from energy-momentum considerations, yield a density of about  $\frac{1}{2}$  normal nuclear density.

The temperatures which are achieved in these proton induced reactions are uniformly lower than those obtained in heavy ion reactions. This is as one would expect since the greater number of NN collisions in a heavy ion reaction presumably leads to greater thermalization. The large difference between pion and proton measured temperatures in heavy ion reactions is not observed in proton induced reactions, perhaps because a hot zone with so few nucleons cannot be divided into a cool exterior and a hot interior. An analysis of  $(p,K)$  reactions would help illuminate this point.

The limiting temperature behavior as a function of bombarding energy which is obtained in this analysis is probably not so much a signature of a phase transition or evidence for an exponentially rising density of states, but likely a consequence of simple NN dynamics which curtails the amount of energy which can be deposited in an average transit of the nucleus by the projectile. More detailed calculations based on the intranuclear cascade approach will be needed to confirm this conclusion.

Nevertheless, several interpretational problems remain with this model. The first is the small number of nucleons in the source, fewer than ten and perhaps fewer than five. The second is the very short lifetime of the source estimated in the classical dense gas calculation, indicating that the source breaks up very rapidly after it has been formed. These calculations suggest that it might be more appropriate to regard the mechanism as one with multiple direct interactions of the incident proton with the target nucleons, followed by final state interactions which smear the energy spectrum of the struck nucleons into an approximately thermal spectrum. This type of picture might be able to accommodate the two observations often used against thermal models:

(i) The  $(p,p')/(p,n)$  ratio measured<sup>51</sup> at 100 MeV is roughly two, as expected in the direct knockout model,<sup>52</sup> but not equal to unity as expected in a thermal model with chemical equilibrium.

(ii) Large analyzing powers are measured<sup>22,53</sup> in the

(p,p') reaction at 800 MeV.

Both of these observations argue that thermalization is incomplete, some vestige of the initial nucleon-nucleon interaction remains in the final state. Perhaps this thermal model analysis discussed above has provided the evidence that with so few nucleons involved in the reaction, and with the reaction occurring over such a short time, complete thermalization is not possible.

#### ACKNOWLEDGMENTS

We wish to thank B. Jennings (TRIUMF) for many useful discussions, and B. Jacak (Michigan State University) for making her thermal model analysis of heavy ion reactions available to us prior to publication. One of us (D.H.B.) wishes to thank the Natural Sciences and Engineering Research Council of Canada for financial support.

- <sup>1</sup>See, for example, R. E. Chrien, T. J. Krieger, R. J. Sutter, M. May, H. Palevsky, R. L. Stearns, T. Kozlowski, and T. Bauer, *Phys. Rev. C* **21**, 1014 (1980).
- <sup>2</sup>D. F. Jackson, *Nucl. Phys.* **A173**, 225 (1971).
- <sup>3</sup>R. D. Amado and R. M. Woloshyn, *Phys. Rev. Lett.* **36**, 1435 (1976).
- <sup>4</sup>S. Frankel, *Phys. Rev. Lett.* **38**, 1338 (1977).
- <sup>5</sup>S. Frankel, *Phys. Rev. C* **17**, 694 (1978).
- <sup>6</sup>For a review, see S. Das Gupta and A. Z. Mekjian, *Phys. Rep.* **72**, 131 (1981).
- <sup>7</sup>G. Ciangaru, C. C. Chang, H. D. Holmgren, A. Nadasen, P. G. Roos, A. A. Cowley, S. Mills, P. P. Singh, M. K. Saber, and J. R. Hall, *Phys. Rev. C* **27**, 1360 (1983).
- <sup>8</sup>R. E. L. Green, D. H. Boal, R. L. Helmer, K. P. Jackson, and R. G. Korteling, *Nucl. Phys.* **A405**, 463 (1983).
- <sup>9</sup>V. I. Komarov, G. E. Kosarev, H. Müller, D. Netzband, V. D. Toneev, T. Stiehler, S. Tesch, K. K. Gudima, and S. G. Mashnik, *Nucl. Phys.* **A326**, 297 (1979).
- <sup>10</sup>S. Frankel, W. Frati, C. F. Perdrisat, and O. B. Van Dyck, *Phys. Rev. C* **24**, 2684 (1981).
- <sup>11</sup>I. Tanihata, Y. Miake, H. Hamagaki, S. Kadota, Y. Shida, R. Lombard, E. Moeller, S. Nagamiya, S. Schnetzer, and H. Steiner, in *Proceedings of the 5th Heavy Ion Summer Study*, Lawrence Berkeley Laboratory Report LBL-12652, Conf.-8105104, 1981; Y. Miake, University of Tokyo Report INS-NUMA-39, 1982.
- <sup>12</sup>D. H. Boal and R. M. Woloshyn, *Phys. Rev. C* **23**, 1206 (1981).
- <sup>13</sup>J. Knoll and J. Randrup, *Phys. Lett.* **103B**, 264 (1981).
- <sup>14</sup>For a review, see S. Nagamiya and M. Gyulassy, in *Advances in Nuclear Science*, edited by J. W. Negele and E. W. Vogt (Plenum, New York, in press), also available as Lawrence Berkeley Laboratory Report LBL-14035, 1982.
- <sup>15</sup>For a review, see J. M. Blatt and V. F. Weisskopf, *Theoretical Nuclear Physics* (Wiley, New York, 1952); I. Dostrovsky, Z. Fraenkel, and P. Rabinowitz, *Phys. Rev.* **118**, 791 (1960), and references therein.
- <sup>16</sup>For a phase space approach to the ejectile energy dependence in inclusive spectra, see J. Knoll, *Phys. Rev. C* **20**, 773 (1979); S. Bohrmann and J. Knoll, *Nucl. Phys.* **A356**, 498 (1981).
- <sup>17</sup>E. Byckling and K. Kajantie, *Particle Kinematics* (Wiley, London, 1973).
- <sup>18</sup>R. Weiner and M. Weström, *Phys. Rev. Lett.* **34**, 1523 (1975); *Nucl. Phys.* **A286**, 282 (1977).
- <sup>19</sup>N. Stelte and R. Weiner, *Phys. Lett.* **103B**, 275 (1981).
- <sup>20</sup>R. Beckmann, S. Raha, N. Stelte, and R. Weiner, *Phys. Lett.* **105B**, 411 (1981).
- <sup>21</sup>J. R. Wu, C. C. Chang, and H. D. Holmgren, *Phys. Rev. C* **19**, 698 (1979).
- <sup>22</sup>G. Roy, L. G. Greeniaus, G. A. Moss, D. A. Hutcheon, R. Liljestrang, R. M. Woloshyn, D. H. Boal, A. W. Stetz, K. Aniol, A. Willis, N. Willis, and R. McCamis, *Phys. Rev. C* **23**, 1671 (1981).
- <sup>23</sup>K. R. Cordell, S. T. Thornton, L. C. Dennis, R. R. Doering, R. L. Parks, and T. C. Schweizer, *Nucl. Phys.* **A352**, 485 (1981).
- <sup>24</sup>S. Frankel, W. Frati, G. Blanpied, G. W. Hoffmann, T. Kozlowski, C. Morris, H. A. Thiessen, O. Van Dyck, R. Ridge, and C. Whitten, *Phys. Rev. C* **18**, 1375 (1978).
- <sup>25</sup>A. Sandoval, H. H. Gutbrod, W. G. Meyer, R. Stock, Ch. Lukner, A. M. Poskanzer, J. Gosset, J.-C. Jourdain, C. H. King, G. King, Nguyen Van Sen, G. D. Westfall, and K. L. Wolf, *Phys. Rev. C* **21**, 1321 (1980); G. D. Westfall (private communication).
- <sup>26</sup>N. A. Burgov, M. K. Blasov, L. S. Vorob'ev, S. A. Gerzon, Yu. T. Kiselev, G. A. Laksin, A. N. Martem'yanov, N. A. Pivnyuk, V. L. Stolin, Yu. V. Terekhov, V. I. Ushakov, and M. M. Chumakov, *Yad. Fiz.* **30**, 720 (1979) [*Sov. J. Nucl. Phys.* **30**, 371 (1979)].
- <sup>27</sup>Y. D. Bayukov, V. I. Efremenko, S. Frankel, W. Frati, M. Gazzaly, G. A. Laksin, N. A. Nikiforov, C. F. Perdrisat, V. I. Tchistilin, and Y. M. Zaitsev, *Phys. Rev. C* **20**, 764 (1979).
- <sup>28</sup>A compilation is given in R. M. DeVries and J. C. Peng, *Phys. Rev. Lett.* **43**, 1373 (1979).
- <sup>29</sup>Heavy ion rapidities and temperatures are from B. V. Jacak (private communication).
- <sup>30</sup>D. R. F. Cochran, P. N. Dean, P. A. M. Gram, E. A. Knapp, E. R. Martin, D. E. Nagle, R. B. Perkins, W. J. Shlaer, H. A. Thiessen, and E. D. Theriot, *Phys. Rev. D* **6**, 3085 (1972).
- <sup>31</sup>C. Gale, A. C. Maso, S. Das Gupta, B. K. Jennings, *Phys. Rev. C* **28**, 164 (1983); C. Gale, M.Sc. thesis, McGill University, 1982.
- <sup>32</sup>S. Tomonaga, *Z. Phys.* **110**, 571 (1936).
- <sup>33</sup>S. Chapman and T. G. Cowling, *The Mathematical Theory of Non-uniform Gases* (Cambridge University, Cambridge, 1939).
- <sup>34</sup>J. O. Hirschfelder, C. F. Curtiss, and R. B. Bird, *Molecular Theory of Gases and Liquids* (Wiley, New York, 1954).
- <sup>35</sup>D. Enskog, *K. Sven. Vetenskapskad. Handl.* **63**, No. 4 (1922).
- <sup>36</sup>H. S. Köhler, *Nucl. Phys.* **A343**, 315 (1980); **A378**, 159 (1982); **A378**, 181 (1982).
- <sup>37</sup>S. Nagamiya, *Phys. Rev. Lett.* **49**, 1383 (1982).
- <sup>38</sup>S. Nagamiya, M.-C. Lemaire, E. Moeller, S. Schnetzer, G. Shapiro, H. Steiner, and I. Tanihata, *Phys. Rev. C* **24**, 971 (1981).
- <sup>39</sup>S. Nagamiya (private communication).
- <sup>40</sup>See H. H. Gutbrod, A. Sandoval, P. J. Johansen, A. M. Poskanzer, J. Gosset, W. G. Meyer, G. D. Westfall, and R. Stock, *Phys. Rev. Lett.* **37**, 667 (1976), and references therein.
- <sup>41</sup>J. I. Kapusta, *Phys. Rev. C* **21**, 1301 (1980).
- <sup>42</sup>See D. H. Boal and M. Soroushian, *Phys. Rev. C* **25**, 1003 (1982).
- <sup>43</sup>For a review of the data, see M. Jacob, in *Proceedings of the 5th Heavy Ion Summer Study*, Lawrence Berkeley Laboratory

- Report LBL-12652, Conf.-8105104, 1981.
- <sup>44</sup>J. G. Zabolitzky and W. Ey, Phys. Lett. 76B, 527 (1978).
- <sup>45</sup>J. W. Van Orden, W. Treux, and M. K. Banerjee, Phys. Rev. C 21, 2628 (1980).
- <sup>46</sup>H. Satz, in *Short Distance Phenomena in Nuclear Physics*, edited by D. H. Boal and R. M. Woloshyn (Plenum, New York, 1983).
- <sup>47</sup>See, for example, D. H. Boal, J. Schachter, and R. M. Woloshyn, Phys. Rev. D 26, 3245 (1982).
- <sup>48</sup>H. Stöcker, G. Buchwald, L. P. Csernai, G. Graebner, J. A. Maruhn, and W. Greiner, Nucl. Phys. A387, 205c (1982).
- <sup>49</sup>R. Hagedorn, Nuovo Cimento Suppl. 3, 147 (1965).
- <sup>50</sup>Particle Data Group, Lawrence Radiation Laboratory Report UCRL-200000NN, 1970.
- <sup>51</sup>B. D. Anderson, A. R. Baldwin, A. M. Kalenda, R. Madey, J. W. Watson, C. C. Chang, H. D. Holmgren, R. W. Koontz, and J. R. Wu, Phys. Rev. Lett. 46, 226 (1981).
- <sup>52</sup>D. H. Boal, Phys. Rev. C 25, 3068 (1982).
- <sup>53</sup>S. Frankel, W. Frati, M. Gazzaly, G. W. Hoffmann, O. Van Dyck, and R. M. Woloshyn, Phys. Rev. Lett. 41, 148 (1978).